

# Mohammad Alsalti

Department of Mechanical Engineering, University of Maryland, 2181 Glenn L. Martin Hall, College Park, MD 20742 e-mail: malsalti@umd.edu

# **Ali Tivay**

Department of Mechanical Engineering, University of Maryland, 2181 Glenn L. Martin Hall, College Park, MD 20742 e-mail: tivay@umd.edu

# Xin Jin

Department of Mechanical Engineering, University of Maryland, 2181 Glenn L. Martin Hall, College Park, MD 20742 e-mail: xjin9891@gmail.com

# George C. Kramer

Department of Anesthesiology, University of Texas Medical Branch, 301 University Boulevard, Galveston, TX 77555 e-mail: gkramer@utmb.edu

# Jin-Oh Hahn<sup>1</sup>

Fellow ASME
Department of Mechanical Engineering,
University of Maryland,
2181 Glenn L. Martin Hall,
College Park, MD 20742
e-mail: jhahn12@umd.edu

# Design and In Silico Evaluation of a Closed-Loop Hemorrhage Resuscitation Algorithm With Blood Pressure as Controlled Variable

This paper concerns the design and rigorous in silico evaluation of a closed-loop hemorrhage resuscitation algorithm with blood pressure (BP) as controlled variable. A lumped-parameter control design model relating volume resuscitation input to blood volume (BV) and BP responses was developed and experimentally validated. Then, three alternative adaptive control algorithms were developed using the control design model: (i) model reference adaptive control (MRAC) with BP feedback, (ii) composite adaptive control (CAC) with BP feedback, and (iii) CAC with BV and BP feedback. To the best of our knowledge, this is the first work to demonstrate model-based control design for hemorrhage resuscitation with readily available BP as feedback. The efficacy of these closedloop control algorithms was comparatively evaluated as well as compared with an empiric expert knowledge-based algorithm based on 100 realistic virtual patients created using a well-established physiological model of cardiovascular (CV) hemodynamics. The in silico evaluation results suggested that the adaptive control algorithms outperformed the knowledge-based algorithm in terms of both accuracy and robustness in BP set point tracking: the average median performance error (MDPE) and median absolute performance error (MDAPE) were significantly smaller by >99% and >91%, and as well, their interindividual variability was significantly smaller by >88% and >94%. Pending in vivo evaluation, model-based control design may advance the medical autonomy in closed-loop hemorrhage resuscitation. [DOI: 10.1115/1.4052312]

### Introduction

Hemorrhage is accountable for approximately 40% of trauma mortality worldwide [1]. Hemorrhage is known to be responsible for the majority of preventable deaths due to traumatic injuries that occur before arrival to receive definitive care at hospitals. It is predicted that approximately 25% of mortality due to hemorrhage may be preventable with early resuscitation and intervention [2]. Hence, early life-saving interventions to treat hemorrhage are a cornerstone to reduce trauma-induced mortality. In fact, shorter prehospital time has been shown to improve survival after traumatic injuries with hemorrhage [3]. However, rapid transport to a hospital equipped with definitive care capability is not always possible. From this standpoint, advanced hemorrhage control capability compatible with prehospital and austere environments may have the potential to improve the mortality rate of hemorrhaging patients.

Hemorrhage is resuscitated in the field by stopping bleeding if possible and then administering volume (i.e., fluids) to the patient to compensate for the volume deficit due to blood loss. In contemporary clinical practice, hemorrhage resuscitation is predominantly manual volume boluses administration by clinicians to a physiological endpoint, e.g., blood pressure (BP) [4]. Such a manual administration of volume can be ad hoc and subjective due to its dependence on individual clinician's experience and

knowledge [5–10] as well as their lapses of vigilance and suboptimal decision-making [11–13]. Noting that the therapeutic range of hemorrhage resuscitation is narrow and the response to hemorrhage resuscitation exhibits a large interindividual variability [14,15], novel capabilities to precisely administer volume (both in terms of timing and dose) are essential in order to drastically advance hemorrhage resuscitation by addressing the abovementioned shortcomings.

A potential solution is to computerize and automate the hemorrhage resuscitation task. Indeed, computerized autonomy can enable dedicated monitoring and treatment of patients with no lapses of vigilance, especially if it is equipped with trustworthy decisionmaking algorithms. Pioneering work to leverage computational autonomy has been reported in the context of closed-loop control of hemorrhage resuscitation [16-22]. These reports strongly suggest the promise of computerized closed-loop administration of hemorrhage resuscitation therapy. Yet, most, if not all, of the existing closed-loop control algorithms have been developed by translating qualitative expert knowledge into empiric rules, including (i) population statistics combined with adaptive error correction and an empiric rule base [17,18,20]; (ii) decision table [16,19]; (iii) proportional-integral-derivative [23,24]; and (iv) fuzzy logic [21,23]. Such rule-based algorithms were shown to be efficacious in pilot in vivo animal and human trials. However, regulatory certification and clinical use of these algorithms require strict understanding of their safety and robustness characteristics as well as limitations, which is usually derived from mathematical analysis in the context of control theory. From this standpoint, qualitative, complex, and nonlinear nature of these rule-based control algorithms, in conjunction with the lack of physiological

<sup>&</sup>lt;sup>1</sup>Corresponding author.

Contributed by the Dynamic Systems Division of ASME for publication in the JOURNAL OF DYNAMIC SYSTEMS, MEASUREMENT, AND CONTROL. Manuscript received August 28, 2020; final manuscript received April 26, 2021; published online October 1, 2021. Editor: Ranjan Mukherjee.

models for stability and robustness analysis of closed-loop control algorithms, may present challenges in conducting such an analysis. In fact, state-of-the-art physiological models involve excessive details, such as ion and protein kinetics, which introduce formidable complexities, making the physiological models less ideal for control design and analysis [25-34]. An alternative approach to overcome this obstacle may be to develop a physiological model amenable to control design (called control design model) and to design a closed-loop control algorithm systematically by exploiting the control design model. This is in fact a well-established procedure in the domain of control systems engineering. Yet, it has not been adopted for the development of closed-loop hemorrhage resuscitation algorithms, because no physiological model appropriate for use in the design and analysis of closed-loop fluid resuscitation controllers exists to the best of our knowledge.

This paper concerns the design of a closed-loop hemorrhage resuscitation algorithm with BP as controlled variable. To the best of our knowledge, this is the first work to demonstrate modelbased control design for hemorrhage resuscitation with readily available BP as feedback. A lumped-parameter control design model relating volume resuscitation input to blood volume (BV) and BP responses was developed and experimentally validated. Then, three alternative adaptive control algorithms were developed using the control design model for hemorrhage resuscitation: (i) model reference adaptive control (MRAC) with BP feedback, (ii) composite adaptive control (CAC) with BP feedback, and (iii) composite adaptive control with BV and BP feedback. The efficacy of these closed-loop hemorrhage resuscitation control algorithms was evaluated as well as compared with an empiric expert knowledge-based algorithm based on 100 realistic virtual patients created using a well-established physiological model of cardiovascular (CV) hemodynamics.

### **Control Design Model**

Model Description. We developed a lumped-parameter control design model representing the dynamical relationship between resuscitation volume versus BV and BP responses (Fig. 1). The control design model is built upon a lumped-parameter model of BV kinetics [35] and extends it to also include the dynamical relationship between BV and BP with a time-varying gain representing the resultant CV actions on BV to elicit BP.

The dynamics of BV is governed by the balance between volume gain (due to resuscitation) and loss (due to, e.g., hemorrhage)

$$\Delta \dot{V}_B(t) = u(t) - v(t) - q(t) \tag{1}$$

where  $\Delta V_B(t) = V_B(t) - V_{B0}$  is the change in BV  $V_B(t)$  from its initial value  $V_{B0}$ , u(t) and v(t) are net fluid gain (i.e., volume resuscitation) and loss (consisting mainly of blood loss due to hemorrhage and urine output), respectively, and q(t) is the intercompartmental fluid exchange [35]. The intercompartmental fluid exchange acts as a critical homeostasis mechanism to compensate for the perturbations in BV, by properly splitting the perturbation

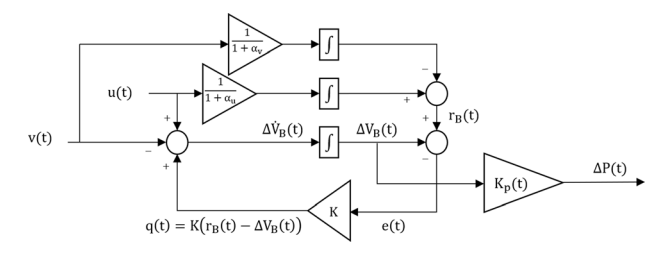


Fig. 1 Lumped-parameter control design model representing the dynamical relationship between fluid resuscitation and BV and BP responses

into intravascular and extravascular compartments. The intercompartmental exchange was modeled as a proportional compensation to regulate BV at a target change in BV in response to BV perturbations

$$q(t) = q(e_B(t)) = K(r_B(t) - \Delta V_B(t))$$
(2)

where  $r_B(t)$  is the target change in BV given by

$$r_B(t) = \frac{1}{1 + \alpha_u} \int_0^t u(\tau) d\tau - \frac{1}{1 + \alpha_v} \int_0^t v(\tau) d\tau$$
 (3)

Here,  $\alpha_u$  and  $\alpha_v$  specify the steady-state split of fluid gain and loss between intravascular and extravascular compartments: BV change due to fluid gain is limited to its  $1/(1+\alpha_u)$  fraction, while the remaining  $\alpha_u/(1+\alpha_u)$  fraction is shifted to the extravascular compartment, and BV change due to fluid loss is limited to its  $1/(1+\alpha_v)$  fraction, while the remaining  $\alpha_v/(1+\alpha_v)$  fraction is shifted from the extravascular compartment. With the assumption that  $\alpha_u$  and  $\alpha_v$  do not substantially change in the timescale of a few hours (which may be supported by our prior work [36,37]), Eq. (3) is a compact phenomenological representation of the real physiology associated with intercompartmental fluid exchange [38]. Combining Eqs. (1)–(3) yields the following linear dynamical equation:

$$\Delta \ddot{V}_B(t) + K \Delta \dot{V}_B(t) = \dot{u}(t) - \dot{v}(t) + K \left( \frac{1}{1 + \alpha_u} u(t) - \frac{1}{1 + \alpha_v} v(t) \right)$$
(4)

The dynamics of BP is related to its BV counterpart through CV functions [39,40]. According to CV physiology, BP (more specifically, mean arterial BP P(t)) is given by the product of cardiac stroke volume (SV;  $V_S(t)$ , which is a function of BV) and arterial elastance (AE;  $(E_A(t))$ 

$$P(t) = V_S(t)E_A(t) = V_S(V_B(t))E_A(t)$$
(5)

Hence, the change in BP from its initial value  $\Delta P(t) = P(t) - P_0$  is given by

$$\Delta P(t) = V_S(t)E_A(t) - V_S(0)E_A(0) = \Delta V_S(t)E_A(t) + \Delta E_A(t)V_S(0)$$
(6)

Assuming that unstressed BV does not substantially change due to volume resuscitation,  $\Delta V_S(t)$  and  $\Delta V_B(t)$  exhibit proportional relationship (given that SV is proportional to stressed BV [40]). In contrast,  $\Delta E_A(t)$  and  $\Delta V_B(t)$  exhibit inversely proportional relationship (due to autonomic-cardiac regulation; Fig. 2) [16]. Hence, simplifying these relationships and denoting  $\Delta V_S(t) = K_{V_S} \Delta V_B(t)$  and  $\Delta E_A(t) = -K_{E_A} \Delta V_B(t)$  yield

$$\Delta P(t) = \left[ K_{V_S} E_A(t) - K_{E_A} V_S(0) \right] \Delta V_B(t) \triangleq K_P(t) \Delta V_B(t)$$
 (7)

where  $K_P(t) = K_{V_S}E_A(t) - K_{E_A}V_S(0)$ . Here, it was assumed that  $\Delta E_A(t)$  and  $\Delta V_B(t)$  are related to each other via a linear gain (which may be valid at least locally). Equation (7) suggests that  $K_P(t)$  accommodates time-varying changes in the relationship between BV and BP due to changes in (i) unstressed BV  $(K_{V_S})$ , (ii) autonomic-cardiac regulation  $(K_{E_A})$ , and (iii) physiological state  $(E_A(t))$ . Finally, combining Eqs. (4) and (7) yields the dynamical relationship between fluid gain/loss and BP

$$\Delta \ddot{P}(t) + K \Delta \dot{P}(t)$$

$$= K_P(t) \left[ \dot{u}(t) - \dot{v}(t) + K \left( \frac{1}{1 + \alpha_u} u(t) - \frac{1}{1 + \alpha_v} v(t) \right) \right]$$
(8)

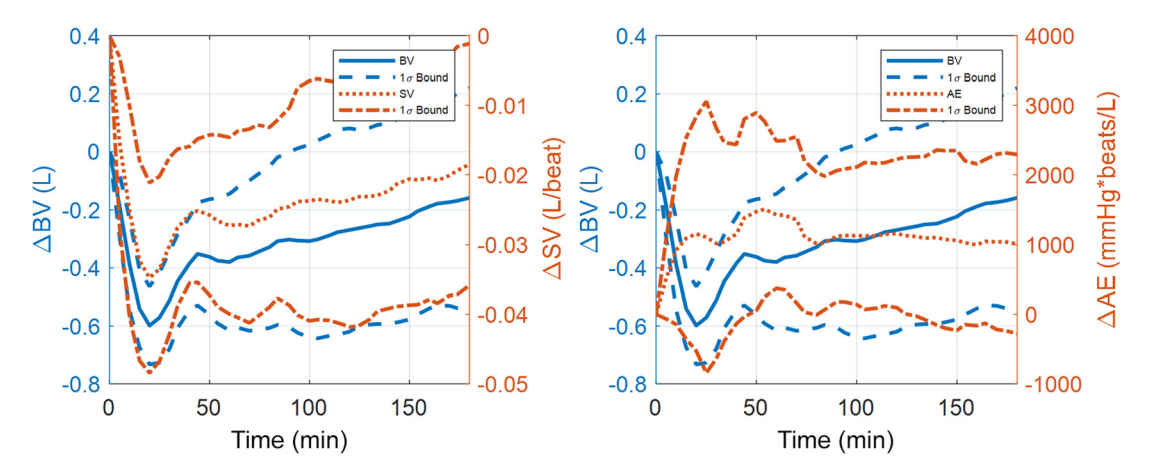


Fig. 2 Experimental observations on the relationships between the changes in SV and AE with respect to the change in BV

In this way, the model structure in Eq. (8) may be well supported by the physical principles underlying volume resuscitation, including (i) the conservation of volume (Eq. (1)), (ii) intercompartmental fluid exchange (Eq. (3)), and (iii) time-varying BV–BP relationship (Eq. (7)), under modest and perhaps justifiable assumptions.

In this work, we will consider BV and BP as measured variables. The rationale underlying BP is its ease of continuous clinical measurement (e.g., with an arterial catheter) despite its complex relationship with BV, while the rationale underlying BV is its potential as an emerging modality for critical care. Indeed, commercialized medical devices have recently appeared in the market to continuously measure blood hematocrit (HCT) [41], based on which BV can be estimated [42].

**Model Validation: Methods.** We examined the validity of the control design model using experimental data collected from 23 sheep undergoing BV perturbations in a prior work [16]. Each animal was subject to (i) controlled hemorrhage of 25 ml/kg over 15 min, (ii) 150-min crystalloid resuscitation starting 30 min after the hemorrhage (the rate of which was determined by a previously investigated closed-loop control algorithm aimed at regulating BP in the sheep [16]), and (iii) controlled hemorrhage of 5 ml/kg over 5 min at 35 min and 55 min after the initial hemorrhage. Measurements made include rates of hemorrhage and urinary output (v(t)) and crystalloid infusion (u(t)), as well as BV (using HCT measurements in conjunction with the indocyanine green dye), BP, and cardiac output.

We validated the control design model on an individual basis. Given that Eq. (8) is a time-varying equation due to  $K_P(t)$ , conventional batch system identification cannot be applied in fitting Eq. (8) to the experimental data. Existing remedies to cope with time-varying parameters (e.g., repetitive generalized least squares across multiple small time intervals followed by averaging [43]) are not suited to our purpose, because they cannot strictly capture the instantaneous value of  $K_P(t)$  at all time instants. Hence, we formulated a novel two-layer optimization problem in Fig. 3. In the upper layer, the parameters  $\alpha_u$ ,  $\alpha_v$ , and K in Eq. (8) are optimized, so that Eq. (8) can best fit the experimental data (BV and BP in particular) in the root-mean-squared sense given  $K_P(t)$ 

$$\Theta^* = \left\{ \alpha_u^*, \alpha_v^*, K^* \right\} \\
= \arg \min_{\Theta} \left( \left\| \frac{\Delta V_B(t) - \Delta \hat{V}_B(t, \Theta)}{\Delta V_{B, \text{max}} - \Delta V_{B, \text{min}}} \right\|_2 + \left\| \frac{\Delta P(t) - \Delta \hat{P}(t, \Theta)}{\Delta P_{\text{max}} - \Delta P_{\text{min}}} \right\|_2 \right) \tag{9}$$

where  $\Delta V_{B,\text{max}}$  and  $\Delta V_{B,\text{min}}$  as well as  $\Delta P_{\text{max}}$  and  $\Delta P_{\text{min}}$  are the maximum and minimum values of  $\Delta V_{B}(t)$  and  $\Delta P(t)$  across the

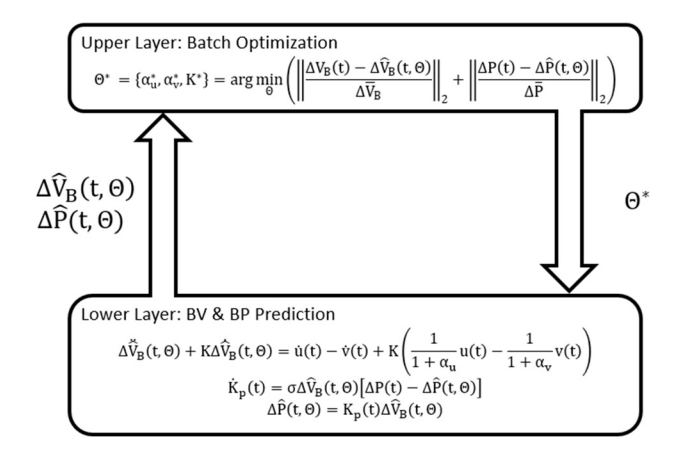


Fig. 3 Two-layer optimization problem formulated to validate control design model in Fig. 1

entire experimental data, respectively, associated with each sheep. To cope with potentially large interindividual variability, we employed multiple initial conditions for  $\alpha_u$ ,  $\alpha_v$ , and K in the physiologically correct (i.e., positive) range in solving Eq. (9), including their group-average values obtained by (i) fitting Eq. (4) to the experimental data on an individual sheep basis to derive subject-specific parameter values and then (ii) averaging them across all the sheep. In the lower layer,  $\Delta \hat{V}_B(t, \Theta)$  is computed using Eq. (4) in conjunction with the values of  $\alpha_u$ ,  $\alpha_v$ , and K furnished by the upper layer, and  $\Delta P(t)$  is computed based on  $\Delta \hat{V}_B(t, \Theta)$  and  $K_P(t)$ , where  $K_P(t)$  is recursively computed based on the gradient-based parameter adaptation law [44,45]

$$\dot{K}_{P}(t) = \sigma \Delta \hat{V}_{B}(t, \Theta) \left[ \Delta P(t) - \Delta \hat{P}(t, \Theta) \right]$$
 (10)

where  $\Delta \hat{V}_B(t,\Theta)$  and  $\Delta \hat{P}(t,\Theta)$  are the changes in BV and BP predicted by the control design model,  $\Delta P(t)$  is the actual change in BP,  $\sigma$  is the adaptation gain, and  $\Theta = \{\alpha_u, \alpha_v, K\}$ . We used the experimental data as the initial conditions for BV  $(V_{B0})$  and BP  $(P_0)$  in solving Eqs. (4), (7), and (10). Hence,  $\hat{V}_B(t,\Theta) = V_{B0} + \Delta \hat{V}_B(t,\Theta)$  and  $\hat{P}(t,\Theta) = P_0 + \Delta \hat{P}(t,\Theta)$ . These two layers are iteratively executed until the parameter estimates converge. We implemented and solved the two-layer optimization problem using MATLAB and its OPTIMIZATION TOOLBOX (MathWorks, Natick, MA).

**Model Validation: Results and Discussion.** Table 1 summarizes the root-mean-squared fitting errors associated with BV, BP, and  $K_P(t)$  (where ground truth  $K_P(t)$  was computed as  $K_P(t)$  =

Table 1 Control design model: experimental validation results

(a) Root-mean-squared fitting errors associated with BV, BP, and $K_P(t)$ in the absolute and percentage sense					
BP BP		$K_P(t)$			
92 ± 39 (ml) (12.8 ± 4.9%)	4.7 ± 2.8 (mm Hg) (8.6 ± 4.7%)	$9.6 \times 10^{-3} \pm 4.7 \times 10^{-3} \text{ (mm Hg/ml)}$ $(7.7 \pm 3.2\%)$			
(b) The values of the parameter esti	imates $\Theta^* = \{\alpha_u^*, \alpha_v^*, K^*\}$				
$\alpha_u^*$	$lpha_ u^*$	$K^* (\min^{-1})$			
$3.3 \pm 1.3$	$1.3 \pm 0.8$	$0.4 \pm 0.2$			

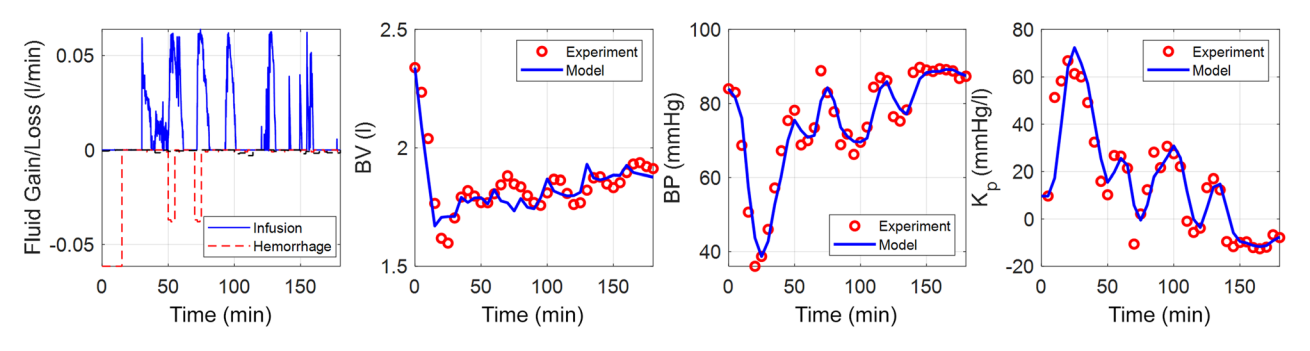


Fig. 4 Representative results obtained from the two-layer optimization in fitting the control design model to experimental data in a sheep ( $\alpha_u^* = 2.73$ ,  $\alpha_v^* = 0.48$ ,  $\kappa' = 0.50$  [min<sup>-1</sup>])

 $\Delta P(t)/\Delta V_B(t)$  from direct measurements of BV  $(V_B(t))$  and BP (P(t)) at each time t), both in the absolute and percentage sense, as well as the values of the parameter estimates  $\Theta^* = \{\alpha_n^*, \alpha_n^*, K^*\}$ . Figure 4 shows a representative example of the results obtained from the two-layer optimization in fitting the control design model to experimental data in a sheep. Once fitted to each sheep, the control design model could accurately replicate the experimental data on BV and BP responses to both hemorrhage and crystalloid resuscitation. In addition, the control design model could track the time-varying parameter  $K_P(t)$ . It is noted that  $K_P(t)$  was estimated using  $\Delta V_B(t,\Theta)$  (i.e.,  $\Delta V_B(t)$ predicted by Eq. (4) but not its measurement) and  $\Delta P(t)$ . Hence, accurate tracking of experimental  $K_P(t)$  shown in Fig. 4 is not trivial. The ability of the control design model to closely reproduce experimental data suggests that it is appropriate to the design of closed-loop control algorithms for hemorrhage resuscitation. In addition, the validation results also suggest that adaptive control may be a reasonable approach to closed-loop control of hemorrhage resuscitation: (i) the intraindividual variability in  $K_P(t)$  can be adequately tracked with a recursive estimation compatible with adaptive control algorithms, and (ii) the interindividual variability in the parameter estimates is substantial (45% for  $\alpha_u^*$  and 67% for  $K^*$ , in terms of the coefficient of variation).

### **Control Design**

The large interindividual parametric variability in the control design model (shown in Control Design Model section) naturally motivates us to explore adaptive control in the design of closed-loop control algorithms for hemorrhage resuscitation. To enable the application of adaptive control theory to hemorrhage resuscitation problem with the plant dynamics given by Eq. (8), we make the following assumptions:

(1) The parameter  $K_P(t)$  is slowly varying and may be regarded as constant for the sake of control design:  $K_P(t) \approx K_P$ . That  $K_P(t) \approx K_P$  is not strictly true due to the autonomic-cardiac

- regulation actions in response to volume resuscitation. However, recursive parameter estimation may still be able to track the time-varying changes in  $K_P(t)$  as shown in Fig. 4.
- (2) The sign of  $K_P$  is known.  $K_P$  is the high-frequency gain of the control design model in Eq. (8). In the physiological context, the sign of  $K_P$  depends on  $K_{V_S}$  and  $K_{E_A}$  (see Eq. (7)). Experimental data suggest that  $K_{V_S} > 0$  while  $K_{E_A} < 0$  on the average. Hence, it is not straightforward to define the sign of  $K_P$ . However, it is well known that the relationship between BV and BP during volume resuscitation is passive (i.e., proportional with positive sign) in the absence of hemorrhage [39]: resuscitation volume increases BV, and BP also increases as BV increases. Hence,  $K_P > 0$  may be safely assumed. A potential drawback is that it restricts the context of use of the closed-loop control algorithm to hemorrhage resuscitation scenarios where blood loss is stopped before resuscitation starts.
- (3) In the adaptive control paradigm, the unknown parameters in the plant dynamics in Eq. (8) can be recursively estimated using the input-output measurements. However, accurate estimation of all these unknown parameters requires the persistence of excitation condition [44,45], which is not easy to anticipate in real-world hemorrhage resuscitation scenarios (simply because the goal of the resuscitation is to save the patient rather than to meet the persistence of exictation condition). In the lack of persistence of excitation in the resuscitation input u(t), the parameter estimates obtained from recursive estimation may suffer from inaccuracy. To overcome this challenge, we treat  $K_P$  as the only unknown parameter in the control design model, while  $\Theta = \{\alpha_u, K\}$  is known a priori. This assumption is justifiable in that (i) current practice of hemorrhage resuscitation consists of iterative administration of multiple boluses, and (ii)  $\Theta = \{\alpha_u, K\}$  may be readily estimated even using the measurements of the bolus input u(t)and BP output  $\Delta P(t)$  associated with a single bolus administration by performing batch system identification of the

control design model in Eq. (8) (see In Silico Evaluation: Results and Discussion section for details) [35].

To achieve the control objective of regulating BP at a desired level, we comparatively investigate three alternatives: (i) MRAC with BP feedback alone, (ii) CAC with BP feedback alone, and (iii) CAC with BP and BV feedback.

Model Reference Adaptive Control With Blood Pressure Feedback. Assuming that (i)  $K_P(t)$  is a constant, i.e.,  $K_P(t) \approx K_P$ , and (ii) hemorrhage has been treated and is absent (v(t) = 0; assuming urine output is negligible), the control design model in Eq. (8) can be written as the following transfer function:

$$G_p(s) = \frac{\Delta P(s)}{U(s)} = K_p \frac{s + \frac{K}{1 + \alpha_u}}{s(s + K)}$$

$$\tag{11}$$

Considering a first-order dynamics as the reference model

$$G_{\text{REF}}(s) = \frac{\Delta P_{\text{REF}}(s)}{\Delta P_{\text{SP}}(s)} = \frac{a_m}{s + a_m}$$
 (12)

where  $\Delta P_{SP}(s)$  is desired change in BP,  $\Delta P_{REF}(s)$  is reference  $\Delta P(t)$  trajectory, and  $a_m$  is the user-specifiable time constant dictating the speed of the reference model. The model reference control law in Eq. (13) yields the closed-loop dynamics in Eq. (12) when applied to Eq. (11) (which can be shown by substituting Eq. (13) into Eq. (11))

$$u(t) = \left(\lambda - \frac{K}{1 + \alpha_u}\right) \frac{u(t)}{p + \lambda} + \frac{1}{K_p} \left\{ \left[\lambda^2 - \lambda K\right] \frac{\Delta P(t)}{p + \lambda} + \left[K - a_m - \lambda\right] \Delta P(t) + a_m \Delta P_{SP}(t) \right\}$$
(13)

where p is the differentiation operator.

Since  $K_p$  is unknown, it must be estimated using a recursive adaptation law. Denoting  $\theta=1/K_p$ ,  $\hat{\theta}(t)=1/\hat{K}_p(t)$  as the estimate of  $\theta$  at time t, and  $\tilde{\theta}(t)=\hat{\theta}(t)-\theta(t)$ , the dynamics of the tracking error  $e(t)=\Delta P(t)-\Delta P_{\rm REF}(t)$  when u(t) in Eq. (13) is implemented with  $\hat{K}_p(t)$  is given by

$$\dot{e}(t) = -a_m e(t) + K_p \tilde{\theta}(t) \left\{ \left[ \lambda^2 - \lambda K \right] \frac{\Delta P(t)}{p + \lambda} + \left[ K - a_m - \lambda \right] \Delta P(t) + a_m \Delta P_{\text{SP}}(t) \right\}$$
(14)

Invoking the following Lyapunov function candidate:

$$V(e(t), \tilde{\theta}(t)) = \frac{1}{2}e^2(t) + \frac{1}{2\gamma_e}K_p\tilde{\theta}^2(t)$$
 (15)

where  $\gamma_e > 0$ , and assuming that perfect knowledge of  $\alpha_u$  and K is available, its time derivative along the trajectory of the error dynamics is given by

$$\dot{V}(e(t),\tilde{\theta}(t)) = e(t)\dot{e}(t) + \frac{1}{\gamma_e} K_p \tilde{\theta}(t) \dot{\tilde{\theta}}(t)$$

$$= -a_m e^2(t) + e(t) K_p \tilde{\theta}(t) \psi(t) + \frac{1}{\gamma_e} K_p \tilde{\theta}(t) \dot{\tilde{\theta}}(t) \quad (16)$$

where  $\psi(t) = [\lambda^2 - \lambda K] (\Delta P(t)/(p + \lambda)) + [K - a_m - \lambda] \Delta P(t) + a_m \Delta P_{\rm SP}(t)$ . Hence, the adaptation law

$$\dot{\hat{\theta}}(t) = -\gamma_e e(t)\psi(t) \tag{17}$$

yields negative semidefiniteness of  $\dot{V}(e(t), \tilde{\theta}(t))$ :  $\dot{V}(e(t), \tilde{\theta}(t))$  =  $-a_m e^2(t) \le 0$ . Consequently,  $V(e(t), \tilde{\theta}(t))$  is bounded. Hence,

the closed-loop dynamics consisting of Eqs. (11), (13), and (17) is globally stable. In turn, the signals e(t),  $\psi(t)$ , and  $\tilde{\theta}(t)$  are bounded, and accordingly  $\dot{e}(t)$  in Eq. (14) is also bounded. As a result,  $\ddot{V}(e(t), \ddot{\theta}(t))$  is bounded, rendering  $\dot{V}(e(t), \bar{\theta}(t))$  uniformly continuous. By invoking Barbalat's lemma, it is concluded that  $\lim_{t\to\infty} \dot{V}(t) = \lim_{t\to\infty} e(t) = 0$ . Hence, we can conclude that the tracking error converges to zero.

Composite Adaptive Control With Blood Pressure Feedback. To enhance the efficacy of estimating  $K_P$ , we explored the use of CAC based on BP feedback, in which the adaptation law in Eq. (17) (which is based on the tracking error e(t)) is augmented by an extra term governed by a prediction error  $\epsilon(t)$  associated with BP. For this purpose, Eq. (11) can be rewritten as follows:

$$\frac{U(s)}{s} = \theta(t) \frac{s+K}{s+\frac{K}{1+\alpha}} \Delta P(s)$$
 (18)

Then, the following prediction error  $\epsilon(t)$  can be defined:

$$\epsilon(t) = \hat{\theta}(t) \frac{p+K}{p+\frac{K}{1+\alpha_u}} \Delta P(t) - \frac{u(t)}{p}$$
 (19)

Using the gradient-based parameter adaptation law [44,45]

$$\dot{\hat{\theta}}(t) = -\gamma_{\epsilon} \epsilon(t) \left[ \frac{p+K}{p+\frac{K}{1+\alpha_{u}}} \Delta P(t) \right]$$
 (20)

where  $\gamma_{\epsilon} > 0$ . Augmenting Eq. (20) to Eq. (17) yields the following CAC law:

$$\dot{\hat{\theta}}(t) = -\gamma_e e(t)\psi(t) - \gamma_\epsilon \epsilon(t) \left[ \frac{p+K}{p+\frac{K}{1+\alpha_u}} \Delta P(t) \right]$$
 (21)

Invoking the Lyapunov function candidate in Eq. (15), and assuming that perfect knowledge of  $\alpha_u$  and K is available, it can be easily shown that its time derivative along the trajectory of the error dynamics in conjunction with the CAC law in Eq. (21) is given by

$$\dot{V}\left(e(t),\tilde{\theta}(t)\right) = -a_m e^2(t) - \frac{\gamma_{\epsilon}}{\gamma_{e}} K_p \tilde{\theta}^2(t) \left[ \frac{p+K}{p+\frac{K}{1+\alpha_u}} \Delta P(t) \right]^2 \le 0$$
(22)

Hence, the argument made on the convergence of the tracking error remains valid for CAC with BP feedback.

Composite Adaptive Control With Blood Pressure and Hematocrit Feedback. To examine the potential value of direct real-time BV measurement (which is not widely used now but may be readily available in the near future with real-time HCT monitoring capability [41]) in addition to BP, we explored the use of CAC based on BV feedback, in which the adaptation law in Eq. (17) (which is based on the tracking error e(t)) is augmented by an extra term governed by a prediction error  $\epsilon(t)$  associated with both BV and BP.

Relative change in BV from its initial value is derived from HCT measurement [42]. Denoting  $\Delta \breve{V}_B(t) = \Delta V_B(t)/V_{B0}$  where  $\Delta \breve{V}_B(t)$  is the relative change in BV and  $V_{B0}$  is the initial BV level, Eq. (4) can be rewritten as follows:

$$\Delta \ddot{V_B}(t) + K \Delta \dot{V_B}(t) = \frac{1}{V_{B0}} \left[ \dot{u}(t) - \dot{v}(t) + K \left( \frac{1}{1 + \alpha_u} u(t) - \frac{1}{1 + \alpha_v} v(t) \right) \right]$$
(23)

And accordingly, the relationship between  $\Delta \breve{V}_B(t)$  and  $\Delta P(t)$  is given by

$$\Delta P(t) = K_p V_{B0} \Delta \breve{V}_B(t) \tag{24}$$

Note that  $V_{B0}$  may be viewed as known a priori along with  $\Theta = \{\alpha_u, K\}$ . Indeed,  $V_{B0}$  may be readily estimated using the measurements of the input u(t) as well as BV output  $\Delta \breve{V}_B(t)$  associated with a single bolus administration by performing batch system identification of the control design model in Eq. (23) [35]. Based on Eq. (24), the following prediction error  $\epsilon(t)$  can be defined:

$$\epsilon(t) = \hat{\theta}(t) \frac{\Delta P(t)}{V_{B0}} - \Delta \breve{V}_B(t)$$
 (25)

Using the gradient-based parameter adaptation law [44,45]

$$\dot{\hat{\theta}}(t) = -\gamma_{\epsilon} \epsilon(t) \frac{\Delta P(t)}{V_{B0}}$$
 (26)

where  $\gamma_{\epsilon} > 0$ . Augmenting Eq. (26) to Eq. (17) yields the following CAC law:

$$\dot{\hat{\theta}}(t) = -\gamma_e e(t) \psi(t) - \gamma_\epsilon \epsilon(t) \frac{\Delta P(t)}{V_{B0}}$$
 (27)

Invoking the Lyapunov function candidate in Eq. (15), and assuming that perfect knowledge of  $\alpha_u$  and K is available, it can be easily shown that its time derivative along the trajectory of the error dynamics in conjunction with the CAC law in Eq. (27) is given by

$$\dot{V}\left(e(t),\tilde{\theta}(t)\right) = -a_m e^2(t) - \frac{\gamma_{\epsilon}}{\gamma_{\epsilon}} K_p \tilde{\theta}^2(t) \left[\frac{\Delta P(t)}{V_{B0}}\right]^2 \le 0$$
 (28)

Hence, the argument made on the convergence of the tracking error remains valid for CAC with BV and BP feedback.

# **Control Algorithm Evaluation**

In Silico Patient Model and Virtual Patient Generation. To evaluate the alternative closed-loop hemorrhage resuscitation control algorithms developed in Control Design section, we used an established and comprehensive physiological model of CV hemodynamics in humans [46]. The physiological model consists of essential components to faithfully describe CV hemodynamics, including: (i) circulatory dynamics in the arteries and the veins, (ii) interaction between intravascular and extravascular compartments, (iii) renal function, (iv) sympathetic and parasympathetic feedback, (v) peripheral autoregulation, and (vi) reninangiotensin control mechanism (Fig. 5). Hence, the physiological model is a powerful tool for simulating short-term and long-term regulation of BV and BP. More specifically, the circulatory dynamics represents the BV dynamics in the intravascular compartment that includes arteries, veins, and the heart as compliant chambers holding the blood. BV and BP are regulated by a suite of autonomic regulation mechanisms including the intercompartmental fluid exchange between intravascular (i.e., blood) and extravascular compartments, the renal function in the kidneys (i.e., urine output), and many BP control functions (such as the autonomic control of cardiac contractility, vascular resistance, and unstressed venous BV, autoregulation as a function of capillary blood flow, and angiotensin control).

We made two extensions to the physiological model to enable the virtual evaluation of the closed-loop control algorithms developed in this work. First, we added the ability to simulate BV changes due to hemorrhage and hemorrhage resuscitation by allowing the blood to be removed from the arterial chamber and the resuscitation fluids to be furnished to the venous chamber.

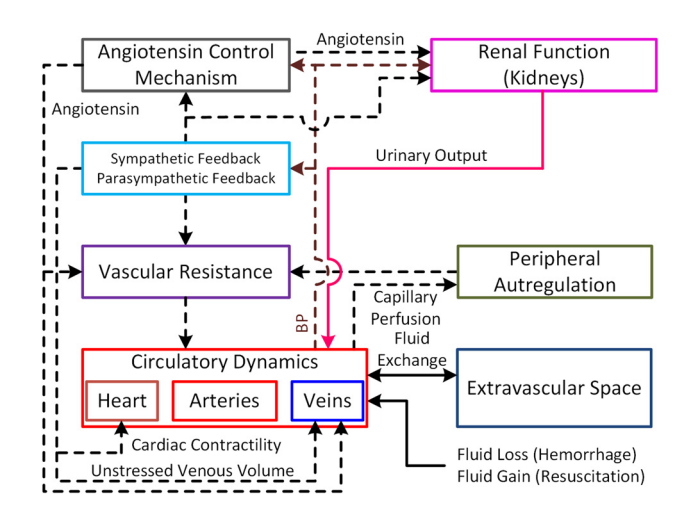


Fig. 5 A physiological model of CV hemodynamics in humans used to create virtual patients

Second, we added the ability to simulate HCT by accounting for the dynamics of plasma volume and red blood cell volume (RBCV) separately, so that BV can be measured from HCT as in the real-world scenarios. Noting that HCT is the fraction of RBCV in BV, the time rate of change in RBCV due to hemorrhage h(t) is given by

$$\Delta \dot{V}_{\rm RBC}(t) = -h(t) \frac{V_{\rm RBC}(t)}{V_B(t)}$$
 (29)

where  $V_{\rm RBC}(t)$  is RBCV, and  $V_B(t) = \Delta V_B(t) + V_{B0}$ . Then, plasma volume  $(V_P(t))$  can be computed by  $V_P(t) = V_B(t) - V_{\rm RBC}(t)$ .

The physiological model is equipped with >40 parameters characterizing the interactions therein to control BP. We selected nine parameters whose variability largely alters BP, including: (i) nominal arterial resistance, (ii) nominal cardiac contractility, (iii) nominal capillary filtration, (iv) nominal venous capacitance, (v) the effect of sympathetic tone on kidney function, (vi) nominal unstressed and total venous BV, and (vii) parameters to characterize angiotensin function. Then, we created a total of 100 virtual patients by randomly sampling these parameters from physiologically reasonable ranges in the vicinity of their respective nominal values, so that BV and BP associated with the virtual patients in the prehemorrhagic state exhibit physiologically adequate values. The resulting virtual patients were associated with prehemorrhage BV range of 4.5–5.5 l and BP range of 70–100 mm Hg.

In Silico Evaluation: Methods and Analysis. To evaluate the closed-loop control algorithms developed in Control Design section, we devised a hemorrhage and resuscitation scenario shown in Fig. 6. In this scenario, the virtual patient is subject to major hemorrhage (2.51). The hemorrhage is treated during the next 120 min. Then, a 0.51 bolus is administered during 30 min. The closed-loop control algorithm is activated 10 min after the bolus is administrated. We executed this scenario in all the 100 virtual patients. Then, we collectively analyzed the efficacy of the closed-loop control algorithms by aggregating the in silico evaluation results obtained from all the virtual patients.

We exploited the BV and BP responses of the virtual patient to the initial bolus to derive the values of  $\Theta = \{\alpha_u, K\}$  and  $K_p$  in Eq. (11), as well as  $V_{B0}$  in Eq. (23). In case of MRAC and CAC with BP feedback, the following optimization problem was solved to yield  $\alpha_u^*$  and  $K^*$  (which were used to implement the control law in Eq. (13) as well as the adaptation laws in Eqs. (17) and (21)) as well as  $K_p^*$  (which was used as the initial condition for the adaptation laws), where the last term is a regularization function based

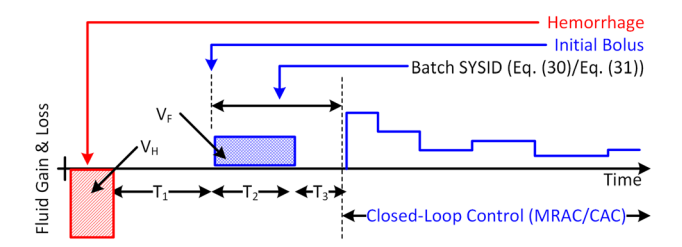


Fig. 6 Hemorrhage and resuscitation scenario used to evaluate the closed-loop control algorithms.  $V_H$ : hemorrhage volume (2.51).  $V_F$ : initial bolus volume (0.51).  $T_1$ : time to treat hemorrhage (120 min).  $T_2$ : time for initial bolus (30 min).  $T_3$ : time interval between initial bolus and closed-loop control (10 min). Hemorrhage duration was 120 min.

on group-average parameter values to robustify the solution (i.e., parameter estimates) against sparse bolus excitation [36]:

$$\left\{\alpha_{u}^{*}, K^{*}, K_{p}^{*}\right\} = \arg\min_{\alpha_{u}, K, K_{p}} \|\Delta P(t) - \Delta \hat{P}(t)\|_{2}$$

$$+ \zeta \left\| \begin{bmatrix} \alpha_{u} \\ K \\ K_{p} \end{bmatrix} - \begin{bmatrix} \bar{\alpha}_{u} \\ \bar{K} \\ \bar{K}_{p} \end{bmatrix} \right\|_{1}$$
(30)

In case of CAC with BV and BP feedback, the following optimization problem was solved to yield  $\alpha_u^*$ ,  $K^*$ , and  $V_{B0}^*$  (which were used to implement the control law in Eq. (13) as well as the adaptation law in Eq. (27)) as well as  $K_p^*$  (which was used as the initial condition for the adaptation law):

$$\begin{aligned}
\left\{\alpha_{u}^{*}, K^{*}, K_{p}^{*}, V_{B0}^{*}\right\} &= \arg\min_{\alpha_{u}, K, K_{p}, V_{B0}} w_{1} \left\| H(t) - \frac{\Delta \hat{V}_{B}(t)}{V_{B0}} \right\|_{2} \\
&+ w_{2} \|\Delta P(t) - \Delta \hat{P}(t)\|_{2} \\
&+ \zeta \left\| \begin{bmatrix} \alpha_{u} \\ K \\ K_{p} \\ V_{B0} \end{bmatrix} - \begin{bmatrix} \bar{\alpha}_{u} \\ \bar{K} \\ \bar{K}_{p} \\ \bar{V}_{B0} \end{bmatrix} \right\|_{1} 
\end{aligned} (31)$$

where H(t) is HCT. Then, each closed-loop control algorithm was implemented using the derived parameter estimates and then executed to achieve the objective of regulating BP at a target set point (which in this work was set at 100 mm Hg in all virtual patients). For all the closed-loop control algorithms, we set the time constant associated with the reference model ( $a_m$  in Eq. (12)) at 15 min.

To compare the efficacy of our closed-loop control algorithms with a benchmark, we evaluated an expert knowledge-based closed-loop hemorrhage resuscitation algorithm reported in a prior work [16,21,47], slightly revised to achieve our 100 mm Hg set point. In brief, the expert knowledge-based algorithm delivers volume at prespecified BP-dependent rates:  $100 \, \text{ml/min}$  per  $70 \, \text{kg}$  body weight if BP <  $40 \, \text{mm}$  Hg, its 80% level if BP is  $41-44 \, \text{mm}$  Hg, 60% level if BP is  $45-49 \, \text{mm}$  Hg, 30% level if BP is  $50-69 \, \text{mm}$  Hg, and 10% level if BP is  $70-99 \, \text{mm}$  Hg. If BP is  $100 \, \text{mm}$  Hg or above, no volume was delivered.

To make the in silico scenario close to the reality, we added measurement noises to BP and HCT signals: BP signal was contaminated with a uniform random noise of 2 mm Hg in magnitude, while HCT signal was contaminated with a uniform random noise of 0.01 in magnitude. The closed-loop control algorithms were equipped with a six-point moving average digital filter to reject the adverse impact of noises. In reality, a BP transducer and a volumetric infusion pump are needed to implement the control loop. Yet, considering that the time constants associated with the BP transducer and the infusion pump are much faster than that of the BV kinetics, dynamic effect of these physical elements was not considered.

In the analysis of the set point tracking and parameter estimation efficacy of the control algorithms, we used the performance error (PE) metrics widely used to assess the performance of computer-controlled automated infusion pumps [48]. We defined the PEs associated with set point tracking and parameter estimation as follows:

$$PE_{e} = \frac{\Delta P_{REF}(t) - \Delta P(t)}{\Delta P(t)} \times 100\%, \quad PE_{\epsilon} = \frac{K_{p}(t) - \hat{K}_{p}(t)}{\hat{K}_{p}(t)} \times 100\%$$
(32)

Using these PEs, we evaluated the efficacy of the closed-loop control algorithms by quantifying, assessing, and comparing the median PE (MDPE), median absolute PE (MDAPE), divergence (DIV, which is a measure of drift in PE), and wobble (which is a measure of intraindividual variability in PE). We used the oneway analysis of variance (ANOVA) with post hoc paired *t*-test to determine the statistical significance in the difference in these measures between the closed-loop control algorithms developed in Control Design section. We used the paired *t*-test to determine the statistical significance in the difference in these measures between CAC with BV and BP feedback (Eqs. (13) and (27)) and the benchmark expert knowledge-based hemorrhage resuscitation algorithm.

In Silico Evaluation: Results and Discussion. Figure 7 presents the resuscitation input (u(t), first row), BV (second row), BP (third row), and finally  $K_p(t)$  and  $\hat{K}_p(t)$  (fourth row) trajectories when (a) MRAC with BP feedback, (b) CAC with BP feedback, and (c) CAC with BV and BP feedback were applied to the nominal virtual patient (BV: 5.01 and BP: 100 mm Hg) subject to the scenario shown in Fig. 6. Table 2 summarizes the PE-based metrics associated with set point tracking and parameter estimation pertaining to all the closed-loop control algorithms (it is noted that the PE-based metrics were computed from the onset of closed-loop control ( $t = 280 \,\mathrm{min}$  in Fig. 6) to  $t = 360 \,\mathrm{min}$  when BP reached the set point). Figure 8 presents the resuscitation input (u(t), first column), BV (second column), and BP (third column)when the expert knowledge-based hemorrhage resuscitation algorithm was applied to the nominal virtual patient (BV: 5.01 and BP: 100 mm Hg) subject to the scenario shown in Fig. 6, while Table 3 summarizes the PE-based metrics associated with set point tracking pertaining to the expert knowledge-based hemorrhage resuscitation algorithm.

All the closed-loop hemorrhage resuscitation algorithms developed in this work performed well in tracking the BP set point (Fig. 7 and Table 2). Regarding the BP set point tracking error, all three closed-loop control algorithms consistently exhibited small bias, inaccuracy, drift, and fluctuations as indicated by small MDPE, MDAPE, divergence, and wobble, respectively, across all the virtual patients. Comparing the three closed-loop control algorithms, CAC with BV and BP feedback was generally superior to MRAC and CAC with BP feedback in all the PE-based metrics. Specifically, the former was superior in terms of MDAPE, divergence, and wobble. In addition, all the metrics associated with the former were more robust in that the spread of the metrics was relatively narrow. However, the difference in these metrics (and accordingly, the overall set point tracking performance) was deemed small from practical perspective. In contrast, regarding the parameter estimation error, CAC with BV and BP feedback exhibited significantly superior performance to MRAC and CAC with BP feedback in all the PE-based metrics (Fig. 7 and Table 2). Indeed, all the PE-based metrics associated with the former were close to zero, whereas the same metrics associated with the latter clearly indicated large bias (negative MDPE, meaning overestimation), poor accuracy (MDAPE being the same as MDPE except sign, meaning again consistently biased overestimation), lack of error convergence (negligible drift with close-to-zero divergence, meaning persistent parameter estimation error), and fluctuation

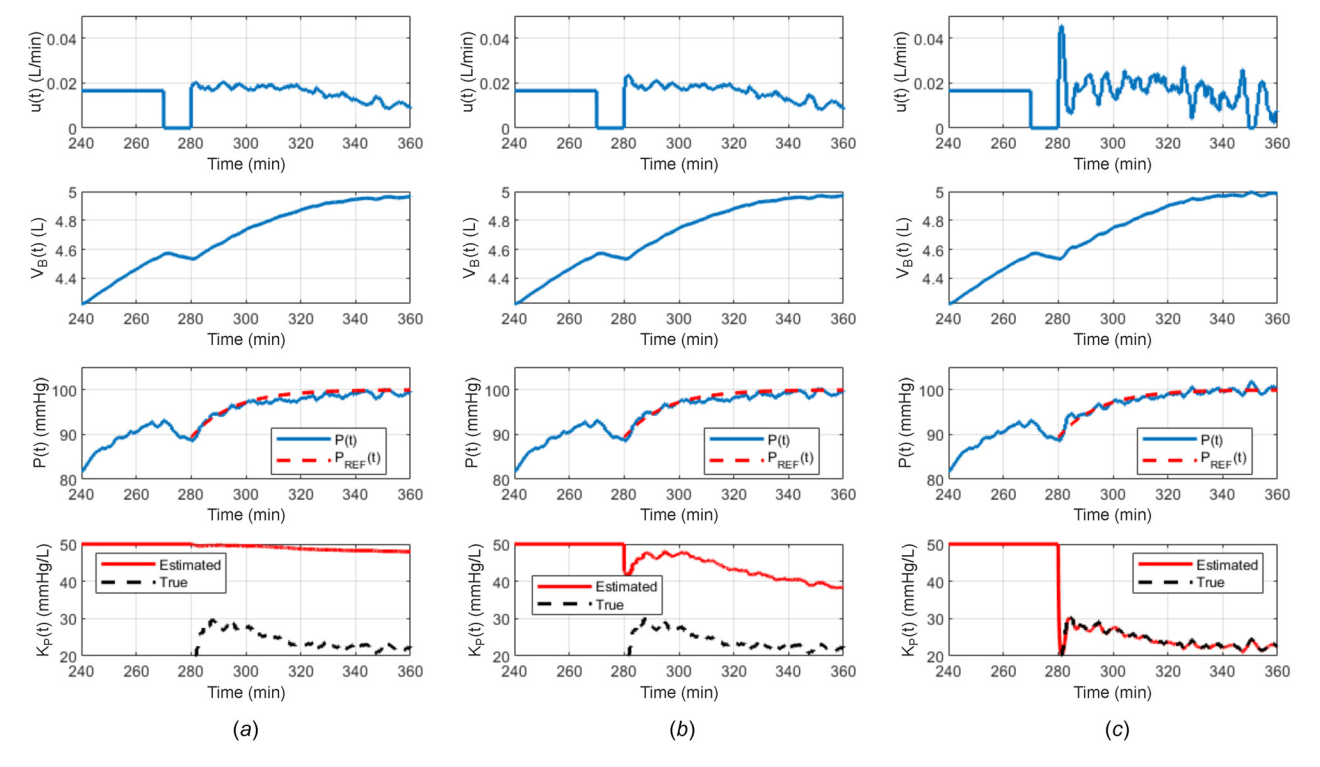


Fig. 7 Representative in silico evaluation results: resuscitation input (u(t)), first row), BV (second row), BP (third row), and  $K_p(t)$  (fourth row) trajectories when (a) MRAC with BP feedback, (b) CAC with BP feedback, and (c) CAC with BV and BP feedback were applied to the nominal virtual patient (BV: 5.01 and BP: 100 mm Hg) subject to the scenario shown in Fig. 6

Table 2 PE-based metrics associated with set point tracking and parameter estimation pertaining to all the closed-loop control algorithms

(a) Set point tracking						
	MDPE (%)	MDAPE (%)	DIV (%/min)	Wobble (%)		
MRAC with BP	$-0.29 \pm 2.51$	$3.32 \pm 0.94$	$-0.15 \pm 0.10$	$3.21 \pm 1.06$		
CAC with BP	$-0.44 \pm 2.18$	$3.35 \pm 0.88$	$-0.19 \pm 0.15^{a}$	$3.45 \pm 1.23$		
CAC with BV and BP	$-0.45 \pm 1.14$	$2.08 \pm 0.58^{a,b}$	$-0.14 \pm 0.07^{b}$	$2.02 \pm 0.57^{a,b}$		
(b) Parameter estimation						
	MDPE (%)	MDAPE (%)	DIV (%/min)	Wobble (%)		
MRAC with BP	$-25.50 \pm 19.35$	$27.70 \pm 16.01$	$-0.05 \pm 0.13$	$1.42 \pm 0.61$		
CAC with BP	$-35.92 \pm 11.13^{a}$	$35.93 \pm 11.13^{a}$	$0.11 \pm 0.14^{a}$	$1.58 \pm 0.49^{a}$		
CAC with BV and BP	$-1.44 \pm 6.38^{a,b}$	$5.54 \pm 3.44^{a,b}$	$-0.03 \pm 0.02^{b}$	$0.00 \pm 0.01^{a,b}$		

<sup>&</sup>lt;sup>a</sup>Significantly different from MRAC with BP (one-way ANOVA).

<sup>&</sup>lt;sup>b</sup>Significantly different from CAC with BP (one-way ANOVA).

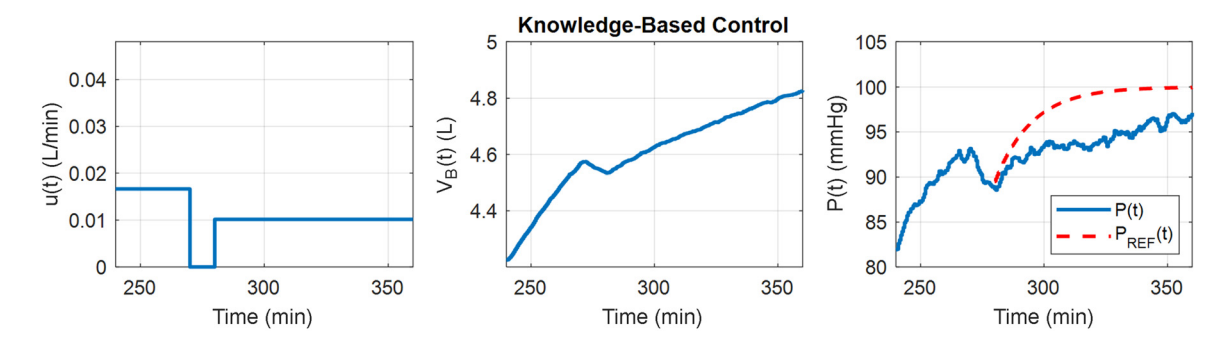


Fig. 8 Representative in silico evaluation results: resuscitation input (u(t), first column), BV (second column), and BP (third column) trajectories when the expert knowledge-based hemorrhage resuscitation algorithm was applied to the nominal virtual patient (BV: 5.01 and BP: 100 mm Hg) subject to the scenario shown in Fig. 6

Table 3 PE-based metrics associated with set point tracking pertaining to the expert knowledge-based hemorrhage resuscitation algorithm

MDPE (%)	MDAPE (%)	DIV (%/min)	Wobble (%)
$22.15 \pm 9.72^{a}$	$22.15 \pm 9.72^{a}$	$0.18 \pm 0.10^{a}$	$1.62 \pm 0.80^{a}$

 $<sup>^{\</sup>mathrm{a}}$ Significantly different from CAC with BV and BP (p < 0.01, paired t-test).

(wobble larger than the former, although small in absolute sense). The notable superiority in parameter estimation performance associated with CAC with BV and BP feedback may be largely attributed to its exploitation of BV measurement. Indeed, the results of bolus-based system identification (Eqs. (30) and (31)) showed that more accurate estimates of the control design model parameters resulted when BV was used in conjunction with BP than when only BP was used: on the average, the errors associated with  $\alpha_u$ , K, and  $K_p$  were 56% and 31%, 176% and 9%, and 12% and 12%, respectively, for Eqs. (30) and (31). In addition, the error associated with  $V_{R0}^*$  for Eq. (31) was generally small (2% on the average). During closed-loop control, the integrity of  $\hat{K}_p(t)$  is largely affected by the accuracy of  $\alpha_u^*$  and  $K^*$  (in all three closed-loop control algorithms) as well as  $\tilde{V}_{B0}^*$  (in CAC with BV and BP feedback), since these parameters are not updated but fixed in implementing the control law in Eq. (13). Considering that the errors associated with these parameters are relatively large in MRAC and CAC with BP feedback than in CAC with BV and BP feedback,  $K_p(t)$  derived from the adaptation laws in Eqs. (17) and (21) was forced to drift away from its actual value in order to compensate for the inaccuracy in  $\alpha_u^*$  and  $K^*$ . On the contrary,  $K_p(t)$ derived from the adaptation law in Eq. (27) was much more accurate by virtue of the superior accuracy in  $\alpha_u^*$ ,  $K^*$ , and  $V_{B0}^*$ . All in all, these results are consistent with the intuitive expectation that supplying more information to adaptive control can enable enhanced set point tracking (despite modest extent in case of this work) and parameter estimation.

In case  $K_n(t)$  was not adapted during closed-loop control (i.e., after "batch system identification" in Fig. 6), set point tracking performance was degraded, especially in terms of robustness, relative to CAC with BV and BP feedback: (i) all the metrics exhibited much larger spread, and (ii) MDAPE and wobble were significantly larger (results not shown). The results demonstrate the advantage of accurate tracking of  $K_p(t)$  in achieving robust set point tracking performance. It is noted that the PE metrics obtained without adapting  $K_p(t)$  were not significantly different from those obtained for MRAC and CAC with BP feedback, which may be attributed to, among other reasons, (i) relatively small changes in  $K_p(t)$  in the in silico evaluation conducted in this work (see Fig. 6) and (ii) inaccurate estimation of  $K_p(t)$  when only BP was used as feedback. However, we anticipate that MRAC and CAC only with BP feedback may still be advantageous in patients undergoing large time-varying changes in  $K_p(t)$ (which needs to be collaborated in a follow-up work).

Compared with the closed-loop control algorithms developed in this work, the expert knowledge-based hemorrhage resuscitation algorithm exhibited very poor set point tracking performance (Fig. 8). In particular, BP response was very slow: it required additional >80 min to reach the set point on the average even with an initial bolus ( $V_F$  in Fig. 6). In the absence of the initial bolus (note that the expert knowledge-based hemorrhage resuscitation algorithm as reported in the prior work is not supposed to require initial bolus), it required additional >140 min to reach the set point on the average (not shown). Accordingly, all the PE-based metrics except wobble were substantially deteriorated compared with the closed-loop control algorithms developed in this work (Table 3): (i) MDPE and MDAPE were both very large, indicating slow BP response; and (ii) divergence was persistently positive, indicating gradual convergence of BP to its set point. Wobble on

the average was smaller in the expert knowledge-based algorithm than in all the closed-loop control algorithms developed in this work, because the volume delivery rate was always constant (at 10 ml/min per 70 kg body weight, since BP was always between 70 and 99 mm Hg in all the virtual patients up to  $t = 360 \,\text{min}$  in Fig. 8). However, the expert knowledge-based hemorrhage resuscitation algorithm behaved like an on-off control once BP reached its set point, switching between 0 ml/min and 10 ml/min (both per 70 kg body weight) susceptibly to the measurement noise associated with BP (not shown). All in all, the slow response associated with the expert knowledge-based algorithm may be enhanced by adjusting its volume delivery rates. However, such enhancement may still necessitate tedious trial-and-error and ad hoc tuning. Furthermore, even the enhanced expert knowledge-based algorithm may not perform as efficaciously as any of the closed-loop control algorithms developed in this work on an individual basis, due to its population-average nature. In this regard, the control design model presented in this work (see Control Design Model section) provides a solid foundation for systematically designing closed-loop control algorithms capable of personalized hemorrhage resuscitation by tailoring its actions to individual patients via online adaptation.

### Conclusion

In this paper, we developed a control-oriented model applicable to systematic design of closed-loop control algorithms for hemorrhage resuscitation and demonstrated its use in the design of three alternative adaptive control algorithms. We experimentally showed that the control design model can replicate BV and BP responses to hemorrhage and hemorrhage resuscitation, thus making it suited to the design of closed-loop control algorithms exploiting BV and BP as controlled variables. Based on an extensive in silico evaluation, we showed that our adaptive control algorithms were significantly superior to an existing expert knowledge-based hemorrhage resuscitation algorithm. Given that the context of use of our closed-loop control algorithms is limited to the scenarios in which hemorrhage has been treated, future work must investigate the development of closed-loop control algorithms equipped with extended context of use.

# Acknowledgment

Any opinions, findings, and conclusions or recommendations expressed in this material are those of the authors and do not necessarily reflect the views of the NSF and ONR.

## **Funding Data**

- Fulbright Program (U.S. Department of State and AMIDEAST).
- U.S. National Science Foundation (NSF, Grant No. CMMI-1760817; Funder ID: 10.13039/100000001).
- U.S. Office of Naval Research (ONR, Grant No. N00014-19-1-2402; Funder ID: 10.13039/100000006).

### References

- Kauvar, D. S., Lefering, R., and Wade, C. E., 2006, "Impact of Hemorrhage on Trauma Outcome: An Overview of Epidemiology, Clinical Presentations, and Therapeutic Considerations," J. Trauma: Inj., Infect., Crit. Care, 60(6), pp. S3–S11.
- [2] Eastridge, B. J., Holcomb, J. B., and Shackelford, S., 2019, "Outcomes of Traumatic Hemorrhagic Shock and the Epidemiology of Preventable Death From Injury," Transfusion, 59(S2), pp. 1423–1428.
- [3] Alarhayem, A. Q., Myers, J. G., Dent, D., Liao, L., Muir, M., Mueller, D., Nicholson, S., 2016, "Time Is the Enemy: Mortality in Trauma Patients With Hemorrhage From Torso Injury Occurs Long Before the 'Golden Hour'," Am. J. Surg., 212(6), pp. 1101–1105.
- [4] Rossaint, R., Bouillon, B., Cerny, V., Coats, T. J., Duranteau, J., Fernández-Mondéjar, E., Filipescu, D., 2016, "The European Guideline on Management of Major Bleeding and Coagulopathy Following Trauma: Fourth Edition," Crit. Care, 20(1), p. 100.

- [5] Bendjelid, K., and Romand, J.-A., 2003, "Fluid Responsiveness in Mechanically Ventilated Patients: A Review of Indices Used in Intensive Care," Intensive Care Med., 29(3), pp. 352–360.
- [6] Rinehart, J., Alexander, B., Manach, Y., Hofer, C., Tavernier, B., Kain, Z. N., and Cannesson, M., 2011, "Evaluation of a Novel Closed-Loop Fluid-Administration System Based on Dynamic Predictors of Fluid Responsiveness: An In-Silico Simulation Study." Crit. Care. 15(6), p. R278.
- An In-Silico Simulation Study," Crit. Care, 15(6), p. R278.

  [7] Le Manach, Y., Hofer, C. K., Lehot, J.-J., Vallet, B., Goarin, J.-P., Tavernier, B., and Cannesson, M., 2012, "Can Changes in Arterial Pressure Be Used to Detect Changes in Cardiac Output During Volume Expansion in the Perioperative Period?," Anesthesiology, 117(6), pp. 1165–1174.

  [8] De Backer, D., and Pinsky, M. R., 2007, "Can One Predict Fluid Responsive-
- [8] De Backer, D., and Pinsky, M. R., 2007, "Can One Predict Fluid Responsiveness in Spontaneously Breathing Patients?," Intensive Care Med., 33(7), pp. 1111–1113.
- [9] Ramsingh, D., Alexander, B., and Cannesson, M., 2012, "Clinical Review: Does It Matter Which Hemodynamic Monitoring System Is Used?," Crit. Care, 17(2), p. 208.
- [10] Marik, P. E., Baram, M., and Vahid, B., 2008, "Does Central Venous Pressure Predict Fluid Responsiveness? A Systematic Review of the Literature and the Tale of Seven Mares," Chest, 134(1), pp. 172–178.
- [11] Qureshi, A. I., Tariq, N., Divani, A. A., Novitzke, J., Hussein, H. H., Palesch, Y. Y., Martin, R., 2010, "Antihypertensive Treatment of Acute Cerebral Hemorrhage," Crit. Care Med., 38(2), pp. 637–648.
- [12] Anderson, C. S., Heeley, E., Huang, Y., Wang, J., Stapf, C., Delcourt, C., Lindley, R., 2013, "Rapid Blood-Pressure Lowering in Patients With Acute Intracerebral Hemorrhage," N. Engl. J. Med., 368(25), pp. 2355–2365.
- [13] Hawryluk, G., Whetstone, W., Saigal, R., Ferguson, A., Talbott, J., Bresnahan, J., Dhall, S., Pan, J., Beattie, M., and Manley, G., 2015, "Mean Arterial Blood Pressure Correlates With Neurological Recovery After Human Spinal Cord Injury: Analysis of High Frequency Physiologic Data," J. Neurotrauma, 32(24), pp. 1958–1967.
- [14] Madigan, M. C., Kemp, C. D., Johnson, J. C., and Cotton, B. A., 2008, "Secondary Abdominal Compartment Syndrome After Severe Extremity Injury: Are Early, Aggressive Fluid Resuscitation Strategies to Blame?," J. Trauma: Inj., Infect., Crit. Care, 64(2), pp. 280–285.
- Inj., Infect., Crit. Care, 64(2), pp. 280–285.
  [15] Hutchings, S. D., Naumann, D. N., Watts, S., Wilson, C., Burton, C., Wendon, J., and Kirkman, E., 2016, "Microcirculatory Perfusion Shows Wide Inter-Individual Variation and Is Important in Determining Shock Reversal During Resuscitation in a Porcine Experimental Model of Complex Traumatic Hemorrhagic Shock," ICMx, 4(1), p. 17.
- [16] Rañe, A. D., Rath, P. A., Michell, M. W., Kirschner, R. A., Deyo, D. J., Prough, D. S., Grady, J. J., and Kramer, G. C., 2004, "Hypotensive Resuscitation of Multiple Hemorrhages Using Crystalloid and Colloids," Shock, 22(3), pp. 262–269.
- [17] Rinehart, J., Le Manach, Y., Douiri, H., Lee, C., Lilot, M., Le, K., Canales, C., and Cannesson, M., 2014, "First Closed-Loop Goal Directed Fluid Therapy During Surgery: A Pilot Study," Ann. Fr. Anesth. Réanim., 33(3), pp. e35–e41.
  [18] Rinehart, J., Lee, C., Canales, C., Kong, A., Kain, Z., and Cannesson, M., 2013,
- [18] Rinehart, J., Lee, C., Canales, C., Kong, A., Kain, Z., and Cannesson, M., 2013, "Closed-Loop Fluid Administration Compared to Anesthesiologist Management for Hemodynamic Optimization and Resuscitation During Surgery: An In-Vivo Study," Anesth. Analg., 117(5), pp. 1119–1129.
- [19] Chaisson, N. F., Kirschner, R. A., Deyo, D. J., Lopez, J. A., Prough, D. S., and Kramer, G. C., 2003, "Near-Infrared Spectroscopy-Guided Closed-Loop Resuscitation of Hemorrhage," J. Trauma, 54(5 Suppl.), pp. S183–S192.
- [20] Rinehart, J., Lilot, M., Lee, C., Joosten, A., Huynh, T., Canales, C., Imagawa, D., Demirjian, A., and Cannesson, M., 2015, "Closed-Loop Assisted Versus Manual Goal-Directed Fluid Therapy During High-Risk Abdominal Surgery: A Case-Control Study With Propensity Matching," Crit. Care. 19(1), p. 94
- Case-Control Study With Propensity Matching," Crit. Care, 19(1), p. 94.

  [21] Marques, N. R., Ford, B. J., Khan, M. N., Kinsky, M., Deyo, D. J., Mileski, W. J., Ying, H., and Kramer, G. C., 2017, "Automated Closed-Loop Resuscitation of Multiple Hemorrhages: A Comparison Between Fuzzy Logic and Decision Table Controllers in a Sheep Model," Disaster Mil. Med., 3(1), p. 1.
- [22] Kramer, G. C., Kinsky, M. P., Prough, D. S., Salinas, J., Sondeen, J. L., Hazel-Scerbo, M. L., and Mitchell, C. E., 2008, "Closed-Loop Control of Fluid Therapy for Treatment of Hypovolemia," J. Trauma: Inj., Infect., Crit. Care, 64(4), pp. S333–S341.
- [23] Libert, N., Chenegros, G., Harrois, A., Baudry, N., Cordurie, G., Benosman, R., Vicaut, E., and Duranteau, J., 2018, "Performance of Closed-Loop Resuscitation of Hemorrhagic Shock With Fluid Alone or in Combination With Norepinephrine: An Experimental Study," Ann. Intensive Care, 8(1), p. 89.

- [24] Bighamian, R., Kim, C.-S., Reisner, A. T., and Hahn, J.-O., 2016, "Closed-Loop Fluid Resuscitation Control Via Blood Volume Estimation," ASME J. Dyn. Syst., Meas., Control, 138(11), p. 111005.
- [25] Tatara, T., and Tashiro, C., 2007, "Quantitative Analysis of Fluid Balance During Abdominal Surgery," Anesth. Analg., 104(2), pp. 347–354.
   [26] Tatara, T., Tsunetoh, T., and Tashiro, C., 2007, "Crystalloid Infusion Rate Dur-
- [26] Tatara, T., Tsunetoh, T., and Tashiro, C., 2007, "Crystalloid Infusion Rate During Fluid Resuscitation From Acute Hemorrhage," Br. J. Anaesth., 99(2), pp. 212–217.
- [27] Carlson, D. E., Kligman, M. D., and Gann, D. S., 1996, "Impairment of Blood Volume Restitution After Large Hemorrhage: A Mathematical Model," Am. J. Physiol.: Regul., Integr. Comp. Physiol., 270(5), pp. R1163–R1177.
- [28] Gyenge, C. C., Bowen, B. D., Reed, R. K., and Bert, J. L., 2003, "Preliminary Model of Fluid and Solute Distribution and Transport During Hemorrhage," Ann. Biomed. Eng., 31(7), pp. 823–839.
- [29] Arturson, G., Groth, T., Hedlund, A., and Zaar, B., 1989, "Computer Simulation of Fluid Resuscitation in Trauma. First Pragmatic Validation in Thermal Injury," J. Burn Care Rehabil., 10(4), pp. 292–299.
- [30] Cervera, A. L., and Moss, G., 1974, "Crystalloid Distribution Following Hemorrhage and Hemodilution: Mathematical Model and Prediction of Optimum Volumes for Equilibration at Normovolemia," J. Trauma Acute Care Surg., 14(6), pp. 506–520.
- [31] Pirkle, J. C., and Gann, D., 1975, "Restitution of Blood Volume After Hemorrhage: Mathematical Description," Am. J. Physiol.: Legacy Content, 228(3), pp. 821–827.
- [32] Hedlund, A., Zaar, B., Groth, T., and Arturson, G., 1988, "Computer Simulation of Fluid Resuscitation in Trauma. I. Description of an Extensive Pathophysiological Model and Its First Validation," Comput. Methods Programs Biomed., 27(1), pp. 7–21.
- [33] Kofránek, J., and Rusz, J., 2010, "Restoration of Guyton's Diagram for Regulation of the Circulation as a Basis for Quantitative Physiological Model Development," Physiol. Res., 59(6), pp. 897–908.
- [34] Pirkle, J. C., 1976, "Mathematical Model of Blood Volume Control After Hemorrhage: Implication for Intravenous Fluid Therapy," Proceedings of the 1976 Summer Computer Simulation Conference, Washington, DC, July 12, pp. 482–485.
- [35] Bighamian, R., Reisner, A. T., and Hahn, J.-O., 2016, "A Lumped-Parameter Subject-Specific Model of Blood Volume Response to Fluid Infusion," Front. Physiol., 7, p. 390.
- [36] Tivay, A., Jin, X., Lo, A. K.-Y., Scully, C. G., and Hahn, J.-O., 2020, "Practical Use of Regularization in Individualizing a Mathematical Model of Cardiovascular Hemodynamics Using Scarce Data," Front. Physiol., 11, p. 452.
- [37] Bighamian, R., Parvinian, B., Scully, C. G., Kramer, G., and Hahn, J.-O., 2018, "Control-Oriented Physiological Modeling of Hemodynamic Responses to Blood Volume Perturbation," Control Eng. Pract., 73, pp. 149–160.
- [38] Guyton, A. C., Taylor, A. E., and Granger, H. J., 1975, Circulatory Physiology II: Dynamics and Control of the Body Fluids, Saunders, Philadelphia, PA.
- [39] Guyton, A. C., 1981, "The Relationship of Cardiac Output and Arterial Pressure Control," Circulation, 64(6), pp. 1079–1088.
- [40] Costanzo, L. S., 2018, *Physiology*, Elsevier, Philadelphia, PA.
- [41] Causey, M. W., Miller, S., Foster, A., Beekley, A., Zenger, D., and Martin, M., 2011, "Validation of Noninvasive Hemoglobin Measurements Using the Masimo Radical-7 SpHb Station," Am. J. Surg., 201(5), pp. 592–598.
- [42] Ewaldsson, C.-A., and Hahn, R. G., 2005, "Kinetics and Extravascular Retention of Acetated Ringer's Solution During Isoflurane or Propofol Anesthesia for Thyroid Surgery," Anesthesiology, 103(3), pp. 460–469.
- [43] Ljung, L., 1999, System Identification: Theory for the User, Prentice Hall, Upper Saddle River, NJ.
- [44] Ioannou, P. A., and Sun, J., 2012, Robust Adaptive Control, Dover Publications, Mineola, NY.
- [45] Slotine, J.-J. E., and Li, W., 1991, *Applied Nonlinear Control*, Prentice Hall, Englewood Cliffs, NJ.
- [46] Guyton, A. C., 1980, Arterial Pressure and Hypertension, Saunders, Philadelphia, PA.
- [47] Vaid, S., Shah, A., Michell, M., Rafie, A., Deyo, D., Prough, D., and Kramer, G., 2006, "Normotensive and Hypotensive Closed-Loop Resuscitation Using 3.0% NaCl to Treat Multiple Hemorrhages in Sheep," Crit. Care Med., 34(4), pp. 1185–1192.
- [48] Varvel, J. R., Donoho, D. L., and Shafer, S. L., 1992, "Measuring the Predictive Performance of Computer-Controlled Infusion Pumps," J. Pharmacokinet. Biopharm., 20(1), pp. 63–94.